



Carbonization of electrospun polyacrylonitrile (PAN)/cellulose nanofibril (CNF) hybrid membranes and its mechanism

Wenlong Xu · Binjie Xin · Xue Yang

Received: 27 August 2019 / Accepted: 16 January 2020 / Published online: 10 February 2020
© Springer Nature B.V. 2020

Abstract Polyacrylonitrile (PAN)/cellulose nanofibril (CNF) based carbon nanofiber membranes were produced by electrospinning and carbonization method, in which the CNF amount was 1 wt%. In order to control the spinning process, the rheological properties of the PAN/CNF suspensions were measured before electrospinning. In addition, the effects of CNF particle size on the structure and properties of carbon nanofiber membranes were investigated systematically by SEM, FTIR and mechanical test. Meanwhile, the reaction mechanism of PAN and PAN/CNF nanofiber membranes in the process of stabilization and carbonization was also fully discussed. The results show that the addition of CNFs can improve the breaking strength and conductivity of PAN carbon nanofiber membrane. Moreover, CNFs also can accelerate the carbonization rate and reduce the reaction conditions of PAN nanofiber membranes. Therefore, CNFs are effective enhancers for PAN based carbon nanofiber membranes.

Keywords Electrospinning · Carbon nanofiber membranes · Polyacrylonitrile · Cellulose nanocrystal · Carbonization

Introduction

As a new type of nanomaterial, carbon fiber has excellent properties, such as electrical conductivity, light weight, high strength, high rigidity, environmental friendliness and low price (Ruiz et al. 2002; Mao et al. 2013; Zou et al. 2006). Therefore, carbon fiber is widely used in electrode material (Jost et al. 2013), transportation, wind power generation and electric power transportation. Since the 1960s, carbon fibers have been developed from a variety of carbon precursors, such as phase asphalt (Wang et al. 2016), phenolic resins (Nam 1999), and cellulose derivatives (Szab et al. 2018), prepared by melt spinning. In the past decade, various manufacturing methods have been employed to produce fibrous carbon materials with diverse structures and properties. Among these preparation methods, chemical vapor deposition (Hu et al. 2019) and arc discharge techniques (Jong et al. 2002) are the most common. However, the preparation process is complicated, and the cost is high.

Preparation of nanofiber membrane materials by electrospinning is one of the most important academic and technical activities in the fields of material science and technology all over the world in recent decades. With the continuous improvement of electrospinning equipment, the spinning cost and the complex process have been greatly reduced. Electrospinning has become one of the main ways to effectively prepare nanofiber materials due to its advantages of simple manufacturing device, low spinning cost, various

W. Xu · B. Xin (✉) · X. Yang (✉)
School of Textiles and Fashion, Shanghai University of
Engineering Science, Shanghai 201620, China
e-mail: xinbj@sues.edu.cn

X. Yang
e-mail: yangxue@sues.edu.cn

spinnable materials and controllable process nowadays. All the continuous fine fibers, with diameters in the range of 10–1000 nm, can be prepared by electrospinning method. Due to the high aspect ratio of the electrospun nanofiber membranes, the specific surface area of the nanofiber membranes is about 1 to 2 orders of magnitude greater than that of ordinary fiber membranes. Recently, there have been many reports about the preparation of carbon nanofiber membranes by electrospinning and carbonization method (Suktha and Sawangphruk 2017). However, the precursor fibers prepared by electrospinning are inferior in strength and irregular in arrangement. Therefore, it is necessary to use reinforcing agent to improve the mechanical properties of the prepared carbon fiber.

Cellulose, the most abundant renewable polymer on the earth, has attracted the researchers' great interest all over the world in recent years, due to its good biodegradability and biocompatibility. However, cellulose is not soluble in the ordinary organic solvents, such as DMF. If it is directly added to the electrospinning dope, the electrospinning pinholes will quickly be clogged and stop the process. The ordinary cellulose is only soluble in the ionic solutions. On the other hand, the addition of the ionic solutions will significantly affect the performance of the electrospinning suspension, such as the rheology and electrical conductivity, which will make the electrospinning suspension difficult to spin smoothly. In addition, the addition of ionic liquid will enhance the water absorption and water permeability of the whole nanofiber membranes to become stronger, which will affect the application of the nanofiber membrane and the subsequent carbonization process. The ordinary cellulose can be converted to highly crystalline nanostructures, termed as cellulose nanofibrils (CNFs), which are obtained by cleaving cellulose fibers along the transverse direction and disrupting amorphous regions under certain conditions (Habibi et al. 2010; Beck et al. 2005; Grunert and Winter 2002). The diameter and length of CNFs range from 5 to 20 nm and 100 nm to several micrometers, respectively, which are significantly affected by the raw cellulose materials and preparation methods (Peresin et al. 2010). As its high specific strength, high crystallinity, and high orientation, as well as its renewability, biodegradability, and eco-friendliness, CNF has attracted considerable attention as a renewable reinforcing nanomaterial for polymer

nanocomposites. As CNF is a kind of nanomaterials, it can be evenly dispersed in DMF or other organic solutions after homogenization treatment to prepare the uniformly electrospinning suspension. Since CNFs are in the nanoscale, they can be normally spun and uniformly dispersed in the nanofiber membrane during the spinning process to achieve a composite effect. Some studies have shown that the carbon nanofiber membranes with added CNFs exhibit good space network structure, high specific breaking strength and modulus (Batista and Drzal 2018; Cao 2014). However, all these studies have been focused on the preparation method, or on the applications of PAN/CNF carbon nanofiber membranes. The carbonization mechanism of PAN/CNF based carbon nanofiber membrane has not been fully researched before. In addition, particle size is one of the most important factors for nanomaterials, which will significantly affect its nanoscale effect. As a kind of nanomaterials, the particle size of CNFs will also affect their enhancement effect. However, to our knowledge, no studies have been reported on the effect of particle size of CNFs on the morphology and properties of PAN based electrospinning carbon nanofiber membrane. Therefore, at the present paper, three kinds of CNFs with different particle size were used as reinforcing agents for PAN nanofiber membranes. After the stabilization process, the PAN/CNF carbon nanofiber membranes were obtained by carbonization at 1200 °C. The effect of particle size of CNFs on the structure and properties of the prepared PAN/CNF carbon nanofiber membranes were fully investigated by SEM, FTIR, TG, rheological and tensile strength test. Moreover, the carbonization mechanism of PAN/CNF nanofiber membranes in each preparation process was fully investigated.

Experimental

Materials

Polyacrylonitrile (PAN, molecular weight 150,000) was purchased from Aladdin chemicals Co., (China), referred as PAN powder. Three kinds of CNFs with 2 μm , 10 μm and 20 μm in length, and 20 nm in diameter were obtained from wood pulp by TMEPO oxidation method, supplied by Woodelfibio Co., (China), referred as freeze-dried CNFs.

Dimethylformamide (DMF) was obtained from Sigma-Aldrich co. and was distilled before use. All materials were vacuum-dried at 60 °C for 24 h to minimize the effects of moisture. The molecular formulas structures of the PAN and CNF were shown in Fig. 1.

Preparation of PAN/CNF electrospinning suspension

The PAN/CNF electrospinning suspensions were prepared as follows. Firstly, 1 g CNF (nanosized of 2 μm , 10 μm and 20 μm in length) was dispersed in 100 ml of DMF solution by magnetically stirring for 2 h. After magnetic stirring, CNFs were evenly dispersed in DMF solution by homogenizer at 23,000 rpm for 30 min. The suspensions of CNFs in DMF were shown in Fig. 2. Then, the PAN powders were added to the above suspension with constant stirring at 200 rpm for 3 h on a magnetic stirrer. The contents of CNFs and PAN were kept 1 wt% and 10 wt%, respectively, in all the electrospinning suspension. The PAN/CNF spinning suspensions were named as PAN/CNF-x, where x (μm) is the size of CNFs in the spinning suspension. In contrast, the neat PAN spinning suspension was also prepared according to the above steps without the addition of CNFs and named as PAN.

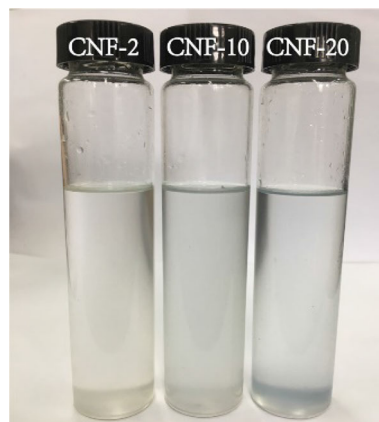


Fig. 2 Photos of the CNF suspensions in DMF

Preparation of PAN/CNF nanofiber membranes

Since this paper mainly focuses on the effect of CNF particle size on the structure and properties of PAN/CNF nanofiber membranes, the effects of parameters during the electrospinning process on the nanofiber membranes were not fully discussed here. After the optimization experiments of spinning process, the optimal preparation process was determined as follows. The neat PAN or PAN/CNF nanofiber membranes were prepared using an electrospinning machine (Laizhou Electronics Co., Ltd.), which consisted of a high voltage–power supply, a syringe as a

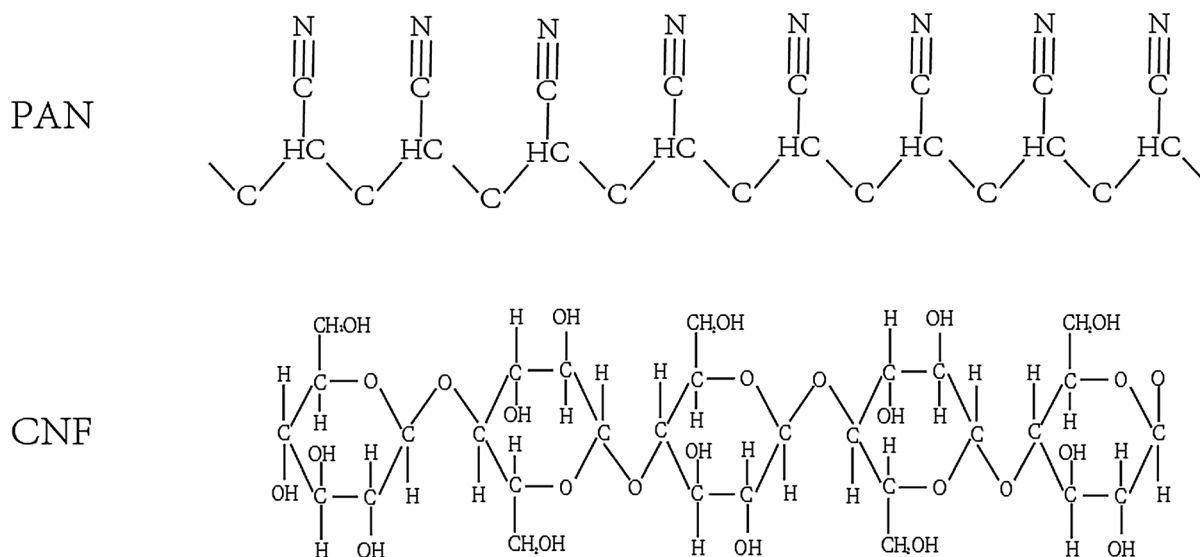


Fig. 1 Molecular formulas structures of the PAN and CNF

spinning dope reservoir, a metallic needle, and a grounded conductive target. During the electrospinning process, the prepared electrospinning suspensions were added to the syringe and moved at a speed of 15 $\mu\text{m}/\text{min}$. A high DC voltage of 20 kV was applied, and the distance from the needle tip to the collector was kept 20 cm. The PAN or PAN/CNF nanofiber membranes were collected on a metal rotating roller at a rotation rate of 40 r/min. During electrospinning, the relative humidity and temperature were 40% and 18 °C, respectively, and the spinning time was 3 h. Before any use, the prepared electrospinning membranes were placed in an oven at 30 °C for 4 h to evaporate much solvent from them. The prepared nanofiber membranes were designed as PAN/CNF-2 membrane, PAN/CNF-10 membrane and PAN/CNF-20 membrane, respectively, depending on the type of spinning suspension. The pure PAN nanofiber membrane was referred as PAN membrane.

Preparation of PAN/CNF carbon nanofiber membranes

The obtained precursor PAN/CNF nanofiber membranes were first conditioned at 80 °C for 1 h to remove the solvent and then stabilized at 280 °C in air for 2 h. Afterwards, the obtained nanofiber membranes were calcined at 1200 °C for 2 h with the heating rate of 5 °C/min under N_2 flow in the tube furnace, and the carbonized nanofiber membranes were denoted as PAN/CNF-2-CM, PAN/CNF-10-CM, and PAN/CNF-20-CM, respectively. The pure PAN carbon nanofiber membrane was prepared the same way as the PAN/CNF carbon nanofiber membranes, which was referred as PAN-CM. The preparation process of the PAN/CNF carbon nanofiber membranes is shown in Fig. 3.

Characterization

Rheological properties

The rheological properties of PAN/CNF spinning suspensions were evaluated using an ARES rheometer. The tests were carried out at room temperature with a 50 mm parallel plate and a gap size of 1 mm. The linear viscoelastic region (LVR) of each sample was determined by performing a strain sweep test at an

oscillation frequency of 100 rad/s. Samples of the electrospinning suspensions were stored in vials, which were sealed with Teflon tape and stored in a dark box at room temperature to prevent solvent evaporation and polymer.

The conductivity of the spinning suspension was measured at room temperature using an EC400 ExStik II conductivity meter.

Scanning electron microscopy

The morphologies of the neat PAN-CM and PAN/CNF-CMs were observed by scanning electron microscopy (SEM, SU8010, Hitachi, Tokyo, Japan). The samples are sputter coated with a thin layer of gold (~ 5 nm), the magnification was set to be 20 K. The diameters of the fibers were measured based on SEM images using image-analysis software (Image Pro Plus 6.0, NIH Image, Bethesda, MD, USA).

Fourier-transform infrared spectroscopy

The chemical structures of the nanofiber membranes were analyzed by Fourier-transform infrared spectroscopy (FTIR, PerkinElmer, Waltham, MA, USA) with KBr crystal in the infrared region 5000–400 cm^{-1} at a resolution of 4 cm^{-1} .

Electrical conductivity

Electrical conductivity of the PAN/CNF-CMs was measured using a four-point probe system with a linear probe head (SZT-2C, Soochow, China). Each membrane was measured five times both in the vertical and horizontal directions, and the average value was used for evaluation. The tests were carried out in a constant temperature and humidity chamber with a temperature of 25 °C and a humidity of 50%.

Mechanical performance

The breaking strength of the prepared nanofiber membranes was measured using a tensile tester. The linear density of the fibers was measured by an on-line vibrometer prior to the tensile test. The samples were cut to a rectangular strip of 50 mm in length and 10 mm in width. The tensile tests were carried out at a strain rate of 50 mm/min. Each membrane was measured five times.

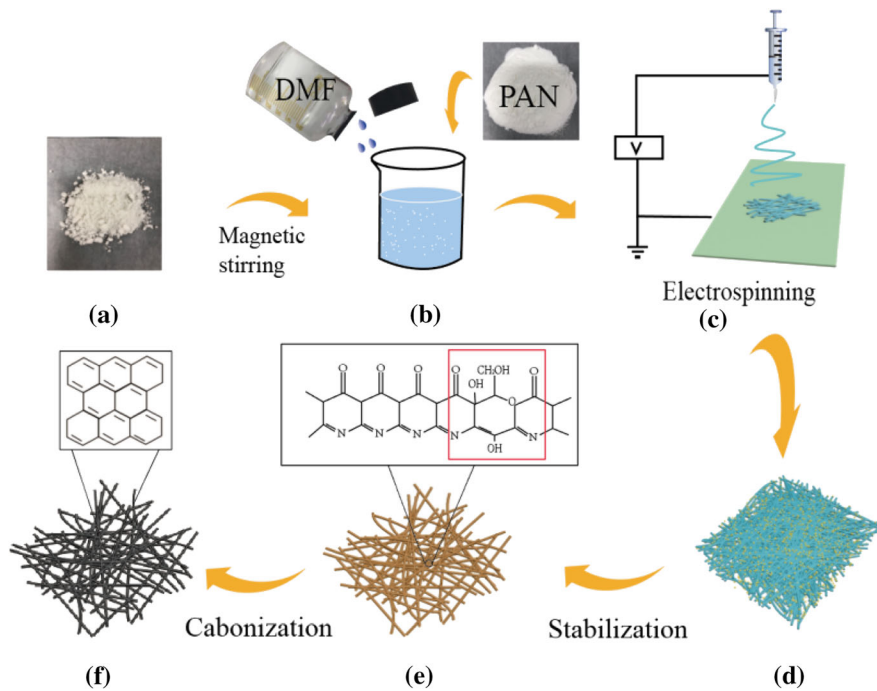


Fig. 3 Schematic illustration of the system and the formation of PAN/CNF carbon nanofiber membranes: **a** is the freeze-dried CNF powders; **b** is the CNF suspensions in DMF; **c** is the PAN/

CNF electrospinning suspensions; **d** is the prepared nanofiber membranes; **e** is the membrane after stabilization and **f** is the PAN/CNF carbon nanofiber membranes

Results and discussion

Characterization of PAN/CNF electrospinning suspensions

The effect of CNF size on the rheological properties and conductivity of PAN/CNF electrospinning

suspensions were measured by rheometer, which was shown in Fig. 4. It can be seen that with the increase of CNF size, the viscosity of electrospinning suspension has a general trend of increasing. Meanwhile, the viscosity of PAN/CNF suspension is increased with aging time, but the changes were very little after 48 h for all the samples. In contrast, the overall trend of neat

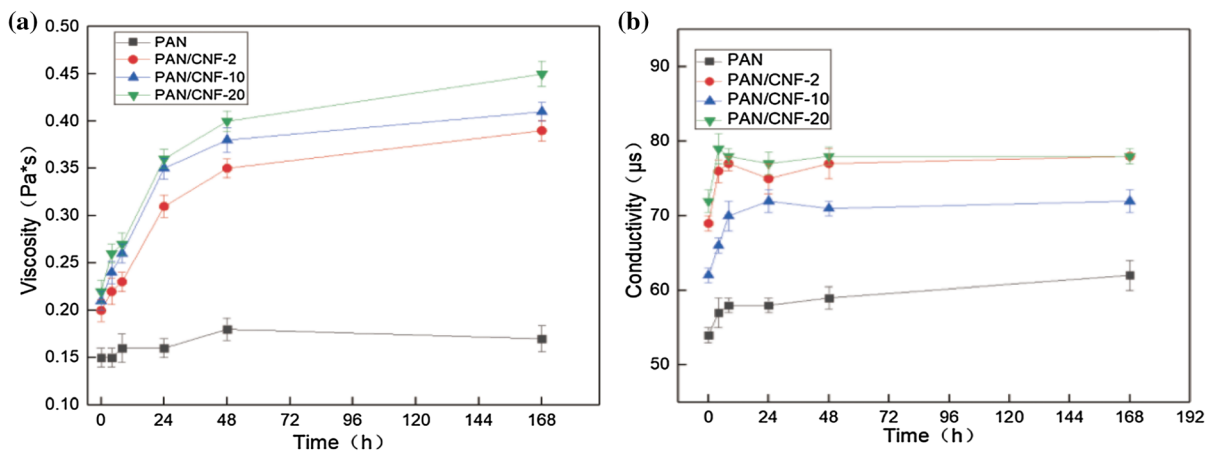


Fig. 4 Viscosity and conductivity of the prepared electrospinning suspensions

PAN electrospinning suspension is fluctuation within a narrow range. The phenomenon that the increase in viscosity with aging time is thought to be the result of polymer-filler interaction, which limits the slip ability of PAN macromolecules. With the increase of the aging time, the number of CNFs adsorbed on the PAN surface is increased, leading to the increase of polymer-filler interaction, which improves the viscosity of PAN/CNF suspensions. In addition, the CNFs with larger particle size have more contact points with PAN macromolecules. This generates more interaction between CNFs and PAN, which lead to the viscosity of PAN/CNF suspensions increase with the increase of size of CNFs.

Conductivity is an important factor for the spinnability of electrospinning suspension, because it determines the rate of charge movement in the suspension, and the discharge of the collected nanofiber membranes. Therefore, it is necessary to measure the conductivity of each electrospinning suspension before spinning. The results of the conductivity tests were shown in Fig. 4. It indicates that the conductivity of the neat PAN spinning suspension is only 54 μs . After the addition of CNFs, the conductivity increases significantly. And the conductivity is increased with the increasing of CNF particle size, which improves from 62 to 73 μs . This might be attributed to the presence of carboxyl group on the surface of CNFs obtained by TEMPO oxidation method. Larger size of CNFs makes more carboxyl groups add to the spinning suspension, leading to a better conductivity. The conductivity values also show an increasing trend with the increasing of ageing time. However, when the ageing time is above 48 h, the change of conductivity is very little.

Surface morphology of PAN/CNF carbon nanofiber membranes

The morphology of the prepared PAN/CNF nanofiber membranes was investigated by SEM images, which was shown in Fig. 5. It displays that all the produced nanofiber membranes show a uniform diameter with no visible beaded structure. The addition of CNFs increases the diameter of PAN/CNF nanofiber membranes obviously. After stabilization and carbonization process, the network structure of PAN and PAN/CNF nanofiber membranes become more regular and orderly, and the surface of the nanofiber membranes

becomes smoother. In addition, some crosslinked structure still can be observed on the nanofiber membranes after stabilization treatment. While, the crosslinked structure disappears after the carbonization treatment.

The statistical chart of the average diameters of PAN/CNF and neat PAN nanofiber membranes at different stages is shown in Fig. 5g. The average diameter of PAN/CNF nanofiber membranes is larger than that of neat PAN nanofiber membranes at each preparation stage. Meanwhile, the diameter of PAN and PAN/CNF nanofiber membranes become smaller and smaller after the stabilization and carbonization treatment. The changes of the PAN/CNF nanofiber membranes diameter might be attributed to the increment of conductivity and viscosity of the electrospinning suspension. The enhancement of the conductivity results in the production of the nanofiber membranes with smaller diameter and more uniform bead-free structure, since the electrospinning suspension jet with higher conductivity is subjected to more tensile under the high electrical field. In addition, the high viscosity can reduce the rapid shape transformation of polymer jets, which lead to the nanofiber membranes with uniform and fine diameters. Moreover, due to the elimination of impurities, the diameter of the neat PAN and PAN/CNF nanofiber membranes gradually reduces during the stabilization and carbonization processes.

Chemical structure analysis of PAN/CNF carbon nanofiber membranes

The effect of CNF particle size on the chemical structure was investigated by FTIR, as shown in Fig. 6. It can be seen that the FTIR spectra of PAN and PAN/CNF nanofiber membranes are very similar. This is because that the characteristics peaks of CNF appear at 3490–3175 cm^{-1} and 1649–1634 cm^{-1} belong to –OH (hydroxyl), at 2900 cm^{-1} and 1382–1375 cm^{-1} belong to –CH, and at 1430–1420 cm^{-1} and 1317 cm^{-1} belong to –CH₂. For PAN, the characteristic peaks are the –CN group (nitrile), which locate at 2243–2240 cm^{-1} . The peaks appear at 2940–2930, 2850, 1450, 1360, and 1050 cm^{-1} in the FTIR curve of the neat PAN membrane, belong to aliphatic –CH, and –CH₂, respectively. Due to the small content of CNFs, the characteristic absorption peaks of CNF are not obvious in the FTIR spectra of PAN/CNF nanofiber

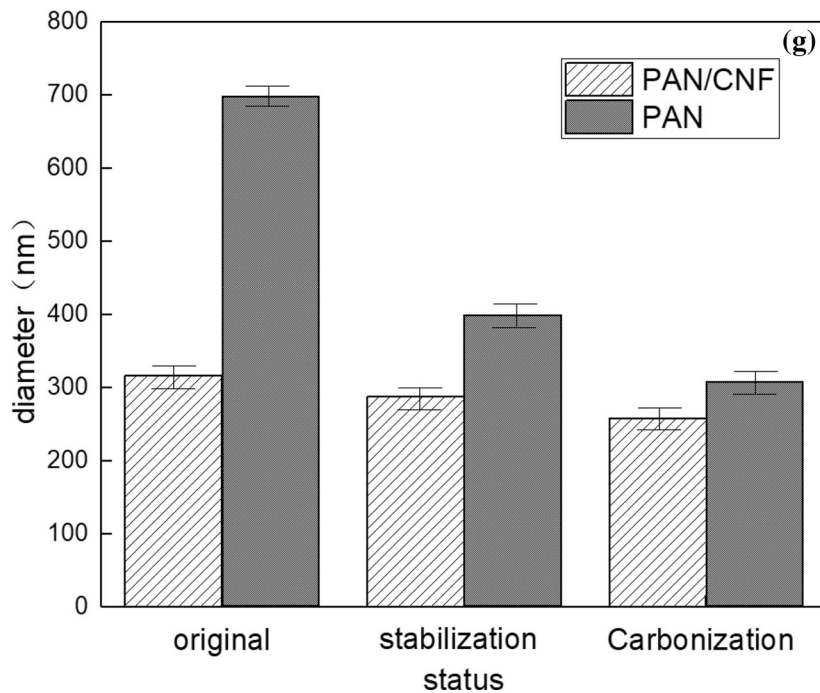
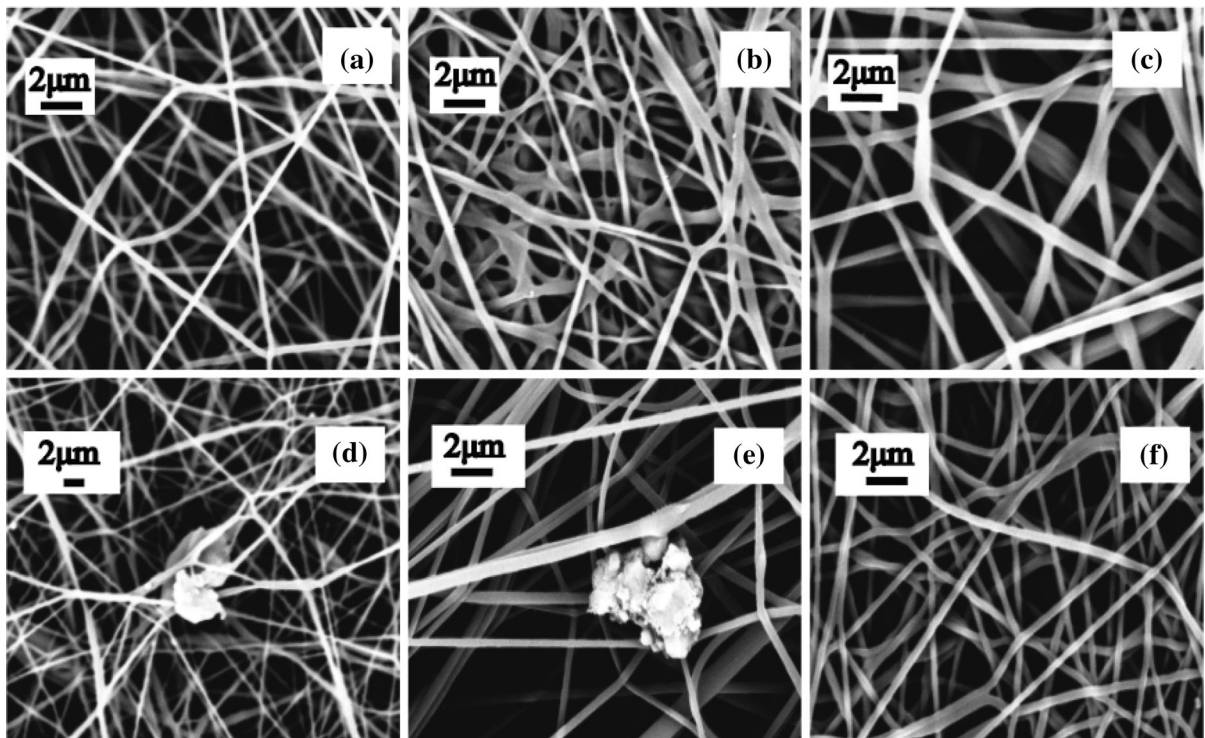


Fig. 5 SEM images of neat PAN and PAN/CNF nanofiber membranes before and after stabilization and carbonization: **a** neat PAN nanofiber membrane; **b** neat PAN nanofiber membrane after stabilization; **c** neat PAN carbon nanofiber

membrane; **d** PAN/CNF nanofiber membrane; **e** PAN/CNF nanofiber membrane after stabilization; **f** PAN/CNF carbon nanofiber membrane; and **g** the average diameter of neat PAN and PAN/CNF carbon nanofiber

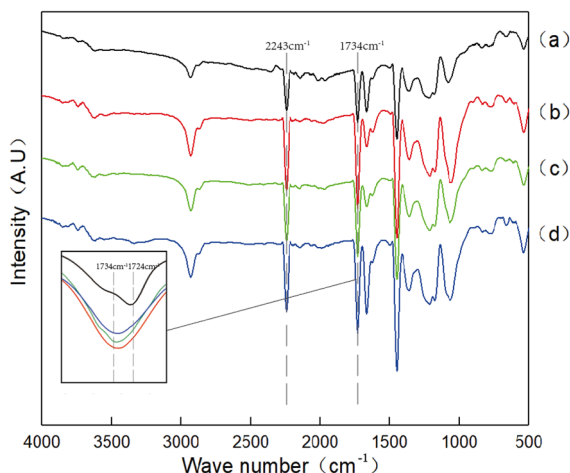


Fig. 6 FTIR spectra of the prepared nanofiber membranes: **a** neat PAN nanofiber membrane; **b** PAN/CNF-2 nanofiber membrane; **c** PAN/CNF-10 nanofiber membrane; **d** PAN/CNF-20 nanofiber membrane

membranes. However, the absorption peaks of $-\text{CH}$ and $-\text{CH}_2$ become sharper attributed to the superposition of the absorption peaks in PAN and CNFs, which indicates the addition of CNFs in the PAN nanofiber membranes. There is no significant difference in the FTIR spectra of the three kinds of PAN/CNF nanofiber membranes, showing that the particle size of CNFs has no effects on the chemical structure of PAN/CNF nanofiber membranes.

The chemical structure of the prepared nanofiber membranes in stabilization at different temperature was analyzed by FTIR, and the results were shown in

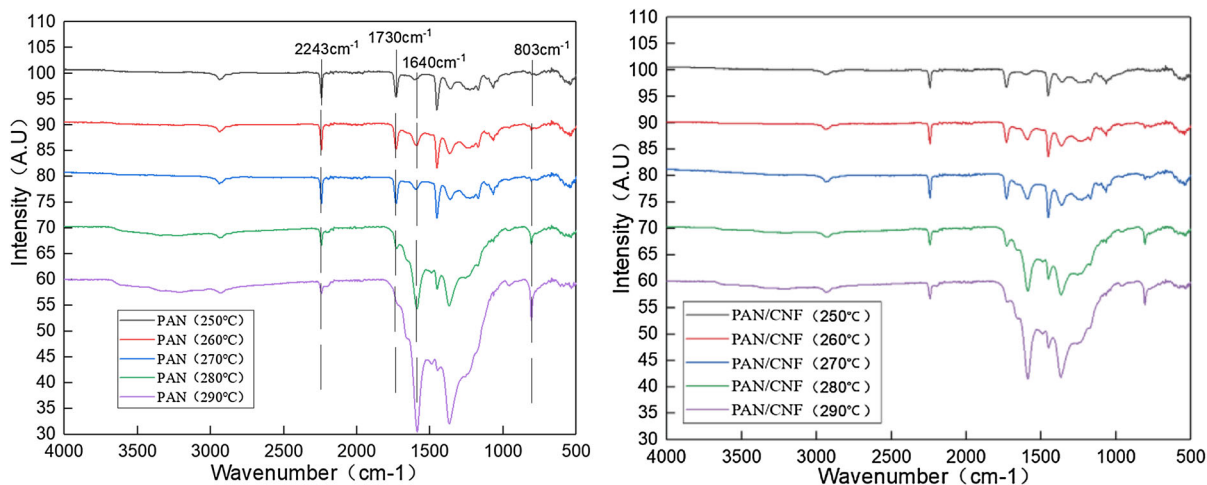


Fig. 7 FTIR spectra of neat PAN and PAN/CNF carbon nanofiber membranes in the stabilization process at different temperatures

Fig. 7. It can be observed that with the increasing of the temperature, the characteristic peak of $-\text{CN}$, which is located at 2243 cm^{-1} , gradually disappears due to the cleavage of the triple bond in the nitrile group. Meanwhile, a distinct characteristic peak gradually appeared at 1640 cm^{-1} attributed to the appearance of the carbon double bond. The ethyl group absorption peak at 1452 cm^{-1} is disappeared due to the generation of double bonds. In addition, with the increase of temperature, the peak of the carbonyl group which locate at 1730 cm^{-1} gradually disappears, while the peak of the para-benzene at 800 cm^{-1} gradually appears. These can be confirmed that the broken nitrile group reconnects to form a cyclic structure during the stabilization process.

For the FTIR spectra of PAN/CNF nanofiber membranes, it is observed that the absorption peaks exhibit the same changes with the increase of stabilization temperature. This is because the particle size has no effect on the chemical structure of PAN/CNF nanofiber membranes. From Fig. 7, it can be seen that the position shift of $-\text{CN}$ peak is not obvious, and no observable new peaks appear in the FTIR curve of PAN/CNF nanofiber membranes, which indicate that no obvious chemical interactions are formed between CNFs and PAN.

As illustrated in Fig. 8 (left), the absorption peaks of $-\text{C}=\text{C}$ double bond and $-\text{C}-\text{C}$ single bond, which are located at 1578 cm^{-1} and 1240 cm^{-1} , appear in the FTIR spectra of neat PAN nanofiber membrane at carbonization temperature of 800 and $900\text{ }^\circ\text{C}$. With

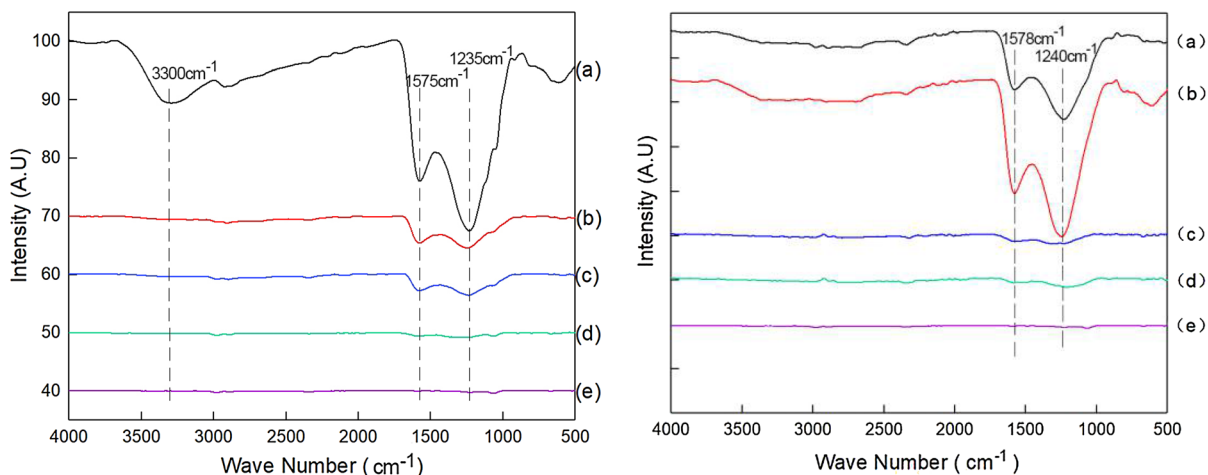


Fig. 8 FTIR spectra of PAN and PAN/CNF carbon nanofiber membranes at different temperatures. PAN/CNF carbon nanofiber membranes (left), neat PAN carbon nanofiber

membrane (right): **a–e** represent carbonization temperature at 800, 900, 1000, 1100 and 1200 °C, respectively

the increase of carbonization temperature, the above absorption peaks decrease gradually. When the carbonization temperature is 1200 °C, there is almost no obvious absorption peaks exist at the above positions, indicating that the degree of carbonization is relatively complete. However, compared with PAN nanofiber membranes, the characteristic absorption peaks of $-C-C$ and $-C=C$ groups decrease significantly at the same carbonization temperatures, except the temperature of 800 °C, in the FTIR spectra of PAN/CNF nanofiber membranes, as shown in Fig. 8 (right). In addition, when the temperature is up to 1100 °C, the characteristic peaks of the functional groups almost disappear completely, showing the completion of carbonization. It can be concluded that the addition of CNFs can reduce the reaction conditions required for the carbonization process.

Electrical conductivity of PAN/CNF carbon nanofiber membranes

The electrical conductivity of PAN/CNF carbon nanofiber membranes was shown in Fig. 9. It exhibits that with the increase of carbonization temperature, the electrical resistance of both neat PAN carbon nanofiber membrane and PAN/CNF carbon nanofiber membranes decreases in general, and their electrical conductivity increases correspondingly. For the neat PAN nanofiber membrane, when the carbonization temperature is lower than 1000 °C, the value of

electrical resistance is very large. When the carbonization temperature is up to 1100 °C, the electrical resistance decreases rapidly, and then becomes stable gradually with the further increase of carbonization temperature. However, compared with the neat PAN nanofiber membrane, the PAN/CNF carbon nanofiber membranes have a much lower electrical resistance at the same carbonization temperature, which indicates that the addition of CNFs can effectively increase the electrical conductivity of the PAN/CNF carbon nanofiber membranes. It can also be seen from Fig. 9 that the size of CNFs has an obvious effect on its electrical conductivity. The PAN/CNF-10 carbon nanofiber membrane exhibits the best conductivity among the three kinds of PAN/CNF carbon nanofiber membranes, which is mainly attributed that it has a better network structure and a more regular orientation.

Figure 9b shows that the electrical resistance of both neat PAN and PAN/CNF carbon nanofiber membranes increase with the increasing of heating rate during carbonization process. Compared with the neat PAN carbon nanofiber membrane, the PAN/CNF carbon nanofiber membranes have a much lower electrical resistance. This might be due to the following two reasons. The first one is that due to the addition of CNFs, the cyclization reaction is accelerated in the stabilization stage, which makes the degree of stabilization increase. The second one is that in the carbonization stage, due to the interaction between

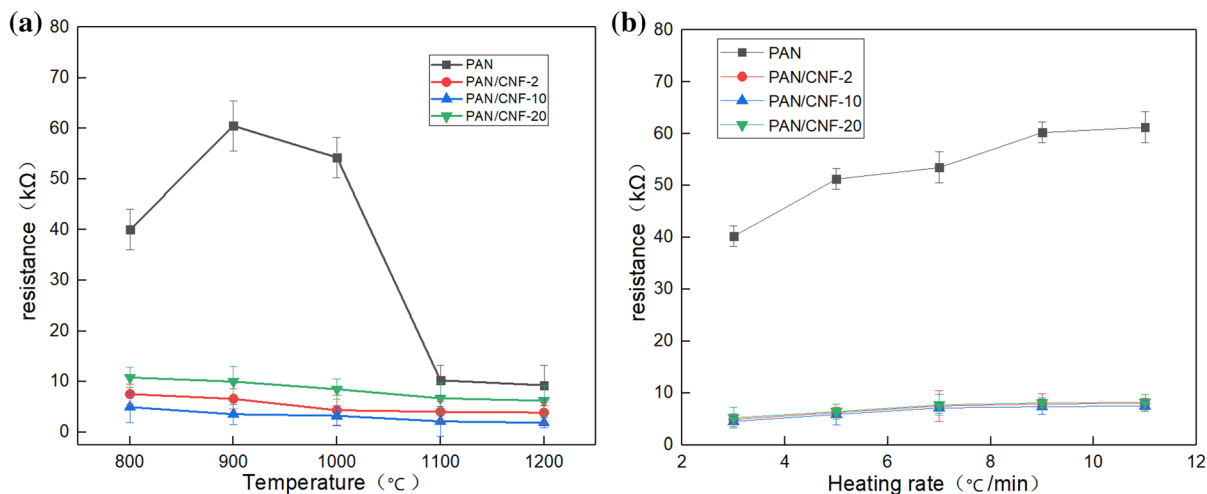


Fig. 9 Electrical resistance of neat PAN and PAN/CNF carbon nanofiber membranes with different temperature and heating rate

the cyclization of CNFs and PAN, the overall cyclization efficiency is better, which accelerates the carbonization process, so that a relatively complete carbonization degree can be achieved at a lower temperature. This is basically consistent with the results obtained from the previous FTIR analysis. In addition, there was no significant difference in the electrical resistance of PAN/CNF carbon nanofiber membranes prepared with three particle sizes of CNFs at the same heating rate, indicating that the particle size has no effect on the electrical conductivity of PAN/CNF carbon nanofiber membranes at different heating rate.

Physical properties of PAN/CNF carbon nanofiber membranes

It can be seen from Fig. 10 that both neat PAN and PAN/CNF carbon nanofiber membranes have a certain mass loss in the carbonization process, and the mass loss of PAN/CNF carbon nanofiber membranes is lower than that of the neat PAN carbon nanofiber membrane. The mass loss of these two substances increases with the increasing of carbonization temperature. In addition, the mass loss of neat PAN carbon nanofiber membrane is more obvious than that of PAN/CNF carbon nanofiber membranes. It is mainly due to the elimination of non-carbon elements and the reorganization of carbon in the carbonization process. Due to the high carbon content of PAN/CNF carbon

nanofiber membranes, the weight loss rate is relatively low.

It can be seen from Fig. 11 that the breaking strength of the prepared carbon nanofiber membranes increases with the increasing of carbonization temperature, and the overall breaking strength of PAN/CNF carbon nanofiber membranes is higher than that of neat PAN carbon nanofiber membrane. The breaking strength of both neat PAN and PAN/CNF samples rises rapidly at the temperature ranging from 800 to 1000 °C. After that, it tends to be stable with further increase of carbonization temperature. This is attributed that since the degree of carbonization is not complete at the temperature of 800–1000 °C, some non-carbon elements and functional groups are not completely decomposed, resulting in the irregular arrangement of carbon elements. Therefore, the breaking strength of the carbon nanofiber membranes is increased obviously with the increasing of carbonization temperature. When the carbonization temperature is more than 1000 °C, most of the non-carbon elements have been eliminated completely, the arrangement and reorganization of carbon elements are basically completed, and the overall orientation of carbon nanofiber membranes is relatively high, resulting in a better strength of carbon nanofiber membrane. Therefore, with the further increase of carbonization temperature, the breaking strength of both neat PAN and PAN/CNF carbon nanofiber membrane changes slowly.

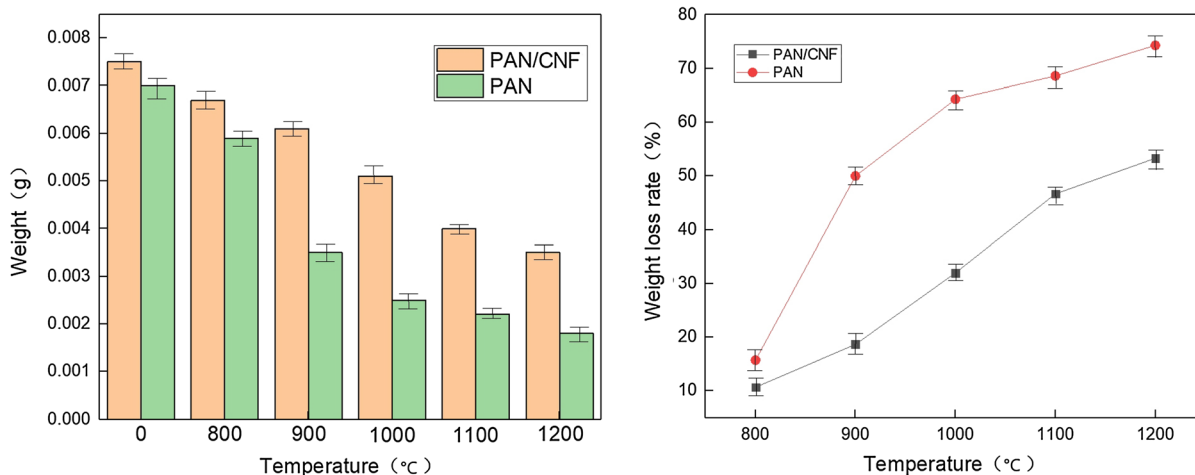


Fig. 10 Neat PAN and PAN/CNF carbon nanofiber membranes mass map (left) and weight loss rate graph (right) at different carbonization temperatures

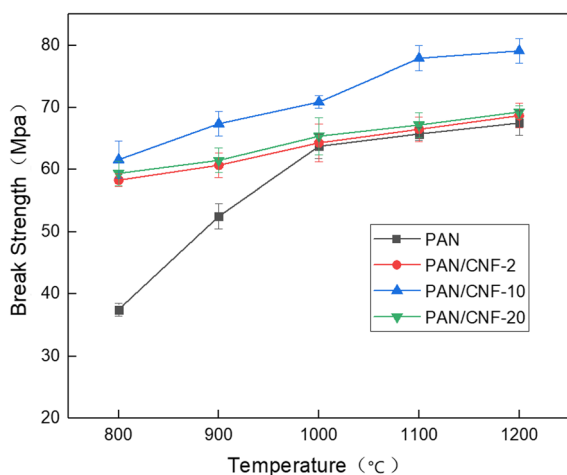


Fig. 11 Breaking strength of neat PAN and PAN/CNF carbon nanofiber membranes at different temperatures

In addition, it also can be seen that the breaking strength of the PAN/CNF carbon nanofiber membranes is improved first and then decreases with the increasing of CNF size. This might be attributed that the number of interactions between CNFs and PAN is increased with the increasing of CNF size. Therefore, the enhancement effect of the CNFs with bigger size is more obvious due to good interfacial adhesion. However, when the size of CNFs is up to 20 μm, the enhancement effect of CNFs reduces. This may be due to the fact that with the increase of CNF size, the interaction between CNFs and CNFs is more pronounced than that of between CNFs and PAN, leading

to the uneven distribution of CNFs in the PAN matrix, which decrease the enhancement effect of CNFs.

Reaction principle analysis of PAN/CNF carbon nanofiber membranes

The preparation of carbon nanofiber membranes involves a heat treatment technology of converting the PAN precursor into carbon nanofiber membranes. This is a complex process in which the temperature is varied at each stage, and nitrogen is used at some stages, while some gases need to be emitted. Therefore, in order to produce the carbon nanofiber membranes with high strength and modulus, it is very important to understand the reaction mechanism of PAN/CNF nanofiber membranes in the process of stabilization and carbonization.

Stabilization

The first stage is pre-oxidative stabilization in the temperature range of 250–280 °C, which mainly occurs the cleavage of the nitrile triple bond and the formation of the heterocyclic six-ring structure, as shown in Fig. 12. After stabilization process, the chemical bond of both neat PAN and PAN/CNF nanofiber membranes has a significant change due to the chemical reaction. Firstly, the characteristic peak of the cyano group located at 2240 cm^{-1} disappears after stabilization, which is caused by the cleavage of

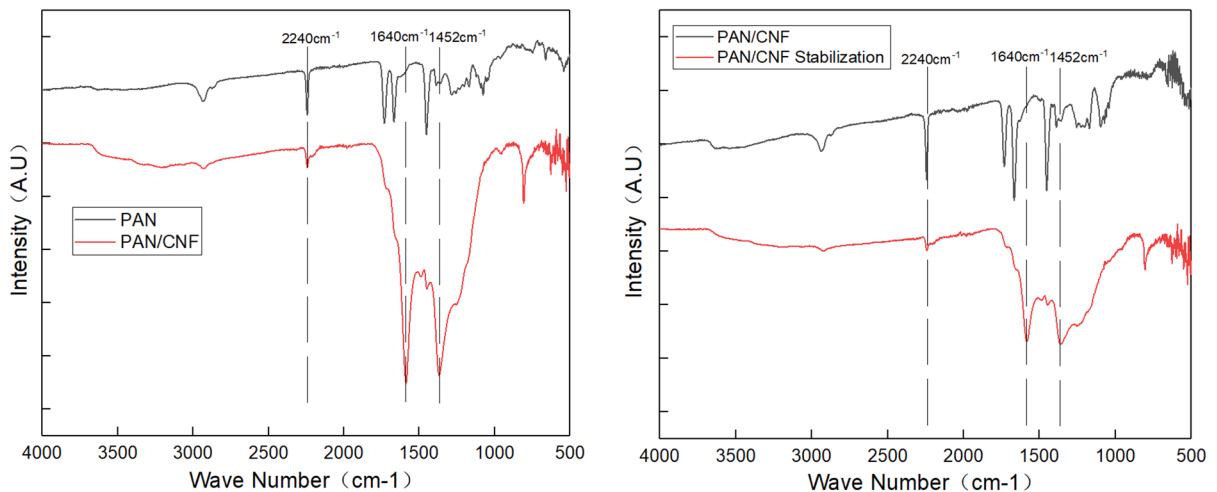


Fig. 12 FTIR spectra of the prepared nanofiber membranes

the carbon–nitrogen triple bond. The characteristic peak of the C=C double bond appears at 1640 cm^{-1} , indicating that the cleavage of the nitrile triple bond initiates the reconnection of the C=C double bond. And the peak of the ethyl group at 1452 cm^{-1} disappears, caused by the generation of C=C double bonds. The formation of the para-benzene peak at 800 cm^{-1} confirms that the fractured nitrile group reconnects to form a ring structure during the stabilization.

In addition, it is also observed from Fig. 12 that after the pre-oxidation stabilization, the FTIR curve of PAN/CNF nanofiber membrane is very similar to that of neat PAN nanofiber membrane. Since CNFs have ring structures, it is speculated that the dehydration reaction of CNFs is the main reaction during the stabilization stage. During the dehydration process, the elimination of the hydroxyl group results in the formation of double bond and conjugated double bond. Therefore, the dehydrated cellulose ring becomes more difficult to cleavage in the subsequent carbonization stage.

According to the above analysis, the reaction mechanism of PAN nanofiber membrane during the stabilization process can be inferred, as shown in Fig. 13. During the stabilization process, PAN nanofiber membrane undergoes the cleavage of the nitrile group and the formation of C=C double bond, leading to the formation of a heterocyclic six-ring structure, which makes the whole structure more stable. During the carbonization process, it can withstand higher

temperature, resulting in the formation of carbon nanofiber membrane finally.

Optical photos of the neat PAN and PAN/CNF carbon nanofiber membranes at different stabilization temperature is shown in Fig. 14. It can be seen that with the increase of the stabilization temperature, the colors of neat PAN nanofiber membrane and PAN/CNF nanofiber membranes become darker and darker, indicating that the non-carbon functional groups are excluded gradually. It is also observed that the stabilization rate of PAN/CNF nanofiber membrane is faster than that of neat PAN nanofiber membrane, which indicates that the addition of CNFs can accelerate the process of stabilization. This is because that during the stabilization process, the addition of CNFs reduces the reaction energy required for the nitrile-based cleavage, promotes the cleavage of the triple bond and the formation of the C=C double bond, which reduce the stabilization conditions of PAN/CNF nanofiber membrane. The more complete the stabilization reaction is, the faster the complete six-ring structure is formed.

Therefore, the reaction mechanism of PAN/CNF nanofiber membrane during the stabilization process can be concluded, which is shown in Fig. 15. For the PAN/CNF nanofiber membrane, the PAN polymer chain undergoes a self-cyclization reaction, while the CNFs mainly occur dehydration reaction during the stabilization process. During the self-cyclization process of the PAN chain, it interacts with the $-\text{CH}$ bond of CNFs to insert a small number of CNFs into the

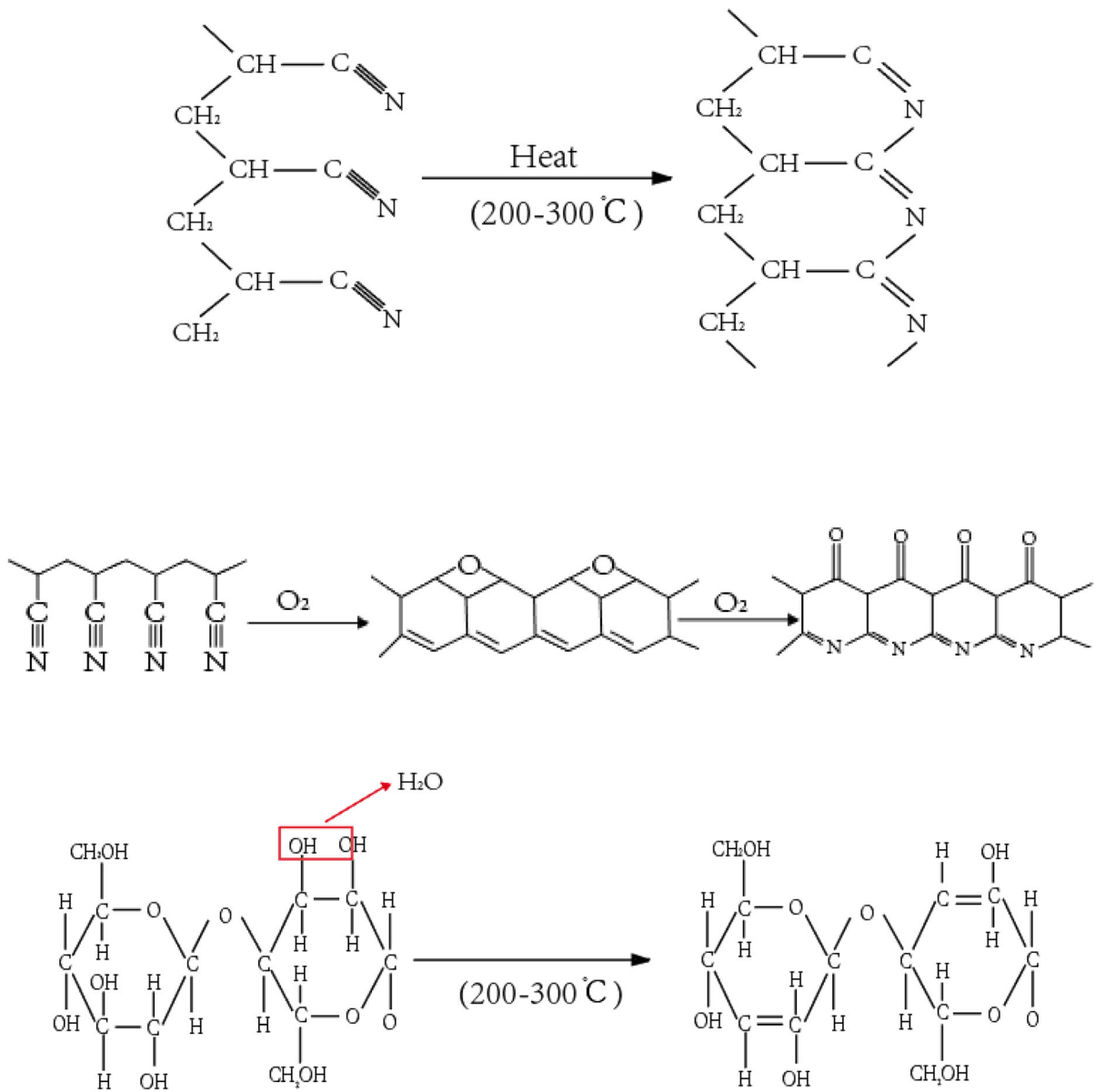


Fig. 13 Reaction mechanism of PAN nanofiber membrane during stabilization process

molecular chain of PAN, and finally forms the structure of PAN/CNF interaction.

Carbonization

In the second stage, carbonization reaction occurs in a nitrogen atmosphere in the temperature range of ~ 1200 °C, in which all heteroatoms are removed as gases, such as N₂, H₂, H₂O, NH₃, and HCN, leading to the formation of haphazardly folded carbon sheets.

It can be observed from the FTIR spectra of Fig. 8 that when the degree of carbonization is complete, there is almost no absorption peaks of other functional groups in the FTIR spectra of the prepared carbon nanofiber membranes. The stabilized nanofiber membranes are heated to 1200 °C in order to be carbonized. During this process, the molecular segments of stabilized PAN nanofiber membrane are decomposed by intramolecular reactions of functional groups. The structure of aromatic rings is formed by dehydration

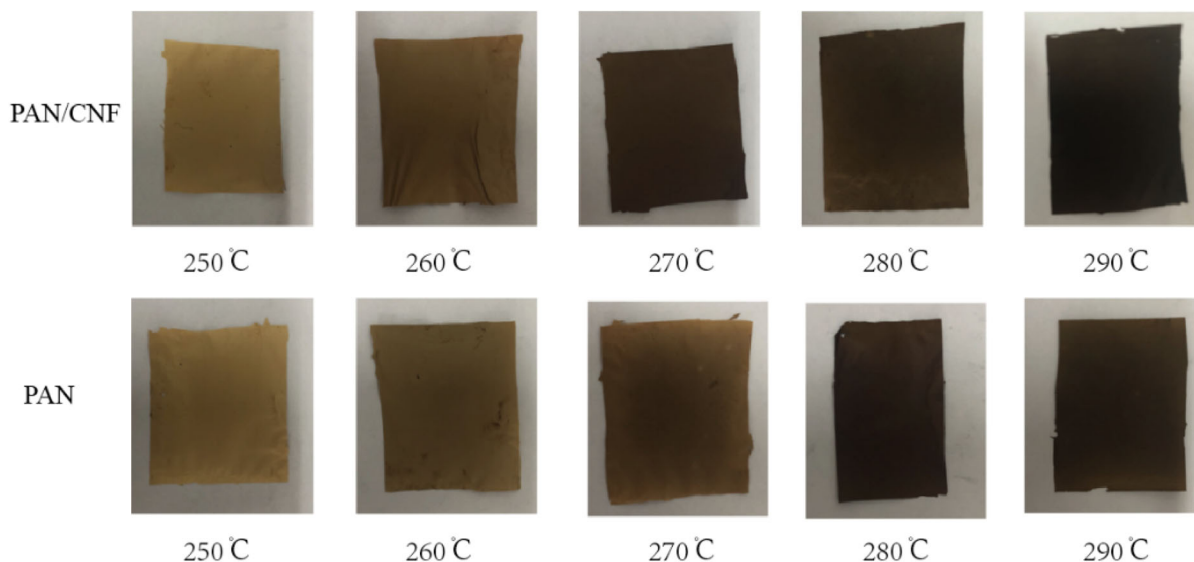


Fig. 14 Optical photos of the neat PAN and PAN/CNF carbon nanofiber membranes at different stabilization temperature

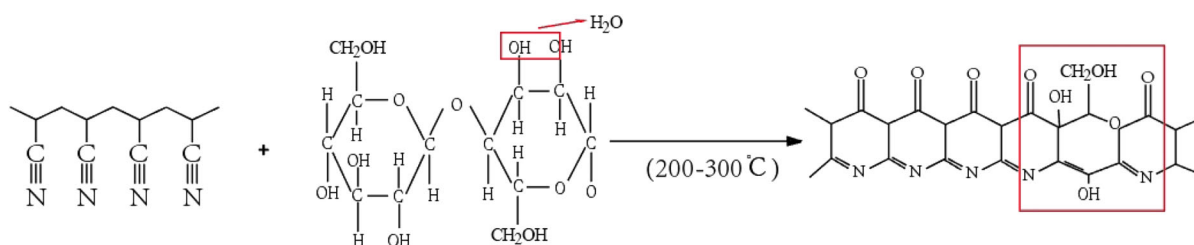


Fig. 15 Reaction mechanism of PAN/CNF nanofiber membrane during the stabilization process

and elimination of hydrogen cyanide during the carbonization process. By comparing the FTIR spectra of PAN and PAN/CNF carbon nanofiber membranes, it can be found that the addition of CNFs can make the PAN/CNF carbon nanofiber membrane achieve a more complete degree of carbonization at a lower reaction condition. Therefore, the presumed reaction mechanism of neat AN nanofiber membrane during carbonization process is shown in Fig. 16.

Since CNFs have ring chemical structures, the main chemical reaction of them are mainly the decomposition of the active functional groups to maintain the stability of the ring structure in the stabilization process. Due to its own active functional groups, it can promote the cyclization process in the stabilization process, thus reducing the temperature and time required for stabilization. In the carbonization process, the ring structure is more likely to form a carbon six

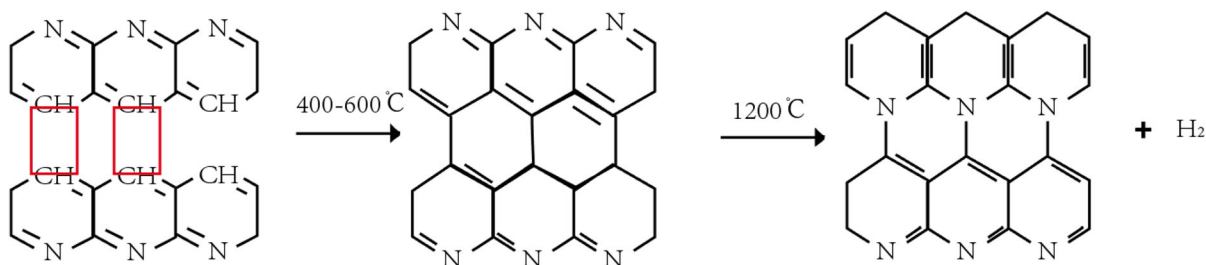


Fig. 16 Reaction mechanism of neat PAN nanofiber membrane during carbonization process

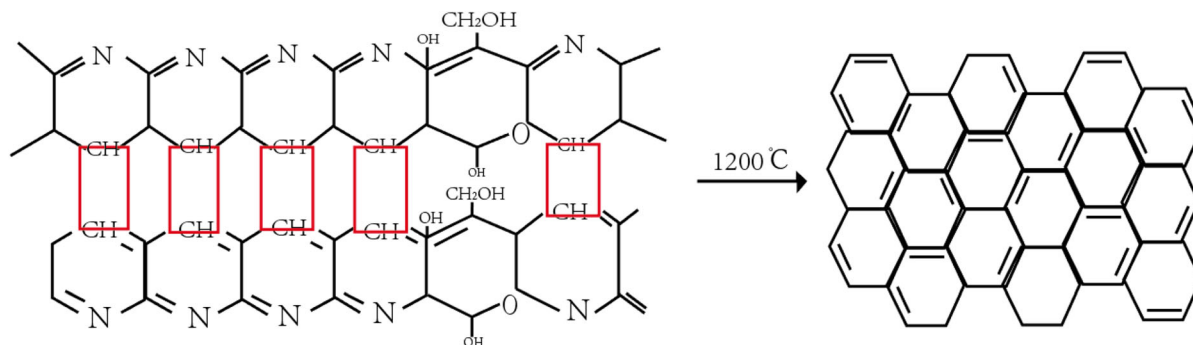


Fig. 17 Reaction mechanism of PAN/CNF nanofiber membrane during carbonization process

ring. At the same time, the reactive functional groups can also react with non-carbon functional groups, which is conducive to the complete rearrangement of carbon elements, thus accelerating the degree of carbonization and making PAN/CNF highly carbonized at a lower temperature.

The carbonization of PAN/CNF nanofiber membrane is a transformation process from a depolymerized structure into a graphite-like layer after the cleavage of polymer chain. Firstly, it forms a ring chain structure, which is interlaced with a certain number of ring structures after stabilization. The $-CH$ bonds between the PAN molecular chains interact with each other at high temperatures to form a sheet-like six-ring graphite structure. Meanwhile, CNFs will be polymerized into monosaccharide derivatives. Then, these intermediates form a fused aromatic structure that release gases containing non-carbon atoms. They also interact with PAN molecules to form a lamellar ring structure. After heat treatment above $800\text{ }^{\circ}\text{C}$, the carbon residue is converted into a more orderly carbon structure under the N_2 atmosphere. The presumed reaction mechanism of PAN/CNF nanofiber membrane during carbonization process is shown in Fig. 17.

Conclusion

In this work, the PAN/CNF carbon nanofiber membranes were prepared by electrospinning method. As the addition of CNFs, the viscosity and conductivity of the PAN/CNF suspensions increased, and both of them were enhanced with the increasing of CNF size. SEM results showed that the average diameter of PAN/CNF nanofiber membranes decreased with the increase of

CNF size, and the diameters of both PAN and PAN/CNF nanofiber membranes decreased after stabilization and carbonization processes. Mechanical performance test results showed that the breaking strength of the PAN carbon nanofiber membrane was improved as the addition of CNFs. FTIR results indicated that no new chemical bonds were formed between CNFs and PAN. After the stabilization process, the characteristic peak of cyano group disappeared, and characteristic peaks of carbon–oxygen double bond and carbon–carbon double bond were generated. Moreover, after the carbonization process, there was almost no absorption peaks of other functional groups in the FTIR spectra of the prepared carbon nanofiber membranes. Finally, the reaction mechanism of PAN/CNF nanofiber membrane can be concluded that PAN mainly undergone the cracking of nitrile triple bonds and an internal cyclization reaction, while CNFs mainly occurred the dehydration cyclization reaction, resulting the formation of a stable ring structure in the stabilization process. While, during the carbonization process, both PAN and CNFs experienced the removal of non-carbon elements in the molecular chain and the formation of regular arrangement of carbon plates. In summary, these results indicate that the addition of CNFs can successfully improve the breaking strength and conductivity of PAN carbon nanofiber membranes. And, it also can promote the cyclization reaction in the stabilization process and reduce the conditions for a complete carbonization reaction. The superior performance of the prepared PAN/CNF carbon nanofiber membranes will have broad application prospects in filtration, sound absorption, heat insulation and many other fields.

Acknowledgments Authors are thankful to the granting financial support under Shanghai University of Engineering and Science Talents Zhi Hong Project (No. 2017RC432017), and National Natural Science Foundation of China (No. 51903152), and Shanghai Science and Technology Talent Project (No. 19YF1417900), and the Research Initiation Funds of Shanghai University of Engineering Science (No. E3-0507-19-05164), and Shanghai Local Capacity-Building Project (No. 19030501200).

Compliance with ethical standards

Conflict of interest No potential conflict of interest was reported by the authors.

References

- Batista MD, Drzal LT (2018) Carbon fiber/epoxy matrix composite interphases modified with cellulose nanocrystals. *Compos Sci Technol* 164:274–281
- Beck S, Roman M, Gray DG (2005) Effect of reaction conditions on the properties and behavior of wood cellulose nanocrystal suspensions. *Biomacromol* 6(2):1048–1054
- Cao Y (2014) Nano-modification for high performance cement composites with cellulose nanocrystals and carbon nanotubes. *Diss Theses Gradworks* 30:1–24
- Grunert M, Winter WT (2002) Nanocomposites of cellulose acetate butyrate reinforced with cellulose nanocrystals. *J Polym Environ* 10(1–2):27–30
- Habibi Y, Lucia LA, Rojas OJ (2010) Cellulose nanocrystals: chemistry, self-assembly, and applications. *Chem Rev* 110(6):3479–3500
- Hu S, Lee CY, Chiu HT (2019) Chemical vapor deposition of carbon nanocoils three-dimensionally in carbon fiber cloth for all-carbon supercapacitors. *ACS Omega* 4(1):195–202
- Jong S, Koo H, Yoo JE (2002) Large scale synthesis of carbon nanotubes by plasma rotating arc discharge technique. *Diam Relat Mater* 11(3–6):914–917
- Jost K, Stenger D, Perez CR (2013) Knitted and screen printed carbon-fiber supercapacitors for applications in wearable electronics. *Energy Environ Sci* 6:2698–2705
- Mao X, Hatton T, Rutledge G (2013) A review of electrospun carbon fibers as electrode materials for energy storage. *Curr Org Chem* 17(13):1390–1401
- Nam SJC (1999) Viscoelastic characterization of phenolic resin-carbon fiber composite degradation process. *J Polym Sci Part B Polym Phys* 37:907–918
- Peresin MS, Habibi Y, Zoppe JO (2010) Nanofiber composites of polyvinyl alcohol and cellulose nanocrystals: manufacture and characterization. *Biomacromol* 11(3):674–681
- Ruiz R, Bedia J, Lallave M (2002) The production of submicron diameter carbon fibers by the electrospinning of lignin. *Carbon* 48(3):696–705
- Suktha P, Sawangphruk M (2017) Electrospinning of carbon-carbon fiber composites for high-performance single coin-cell supercapacitors: effects of carbon additives and electrolytes. *Ind Eng Chem Res* 7:02797
- Szab L, Sari I, Naohiro K (2018) Carbon fibre reinforced cellulose-based polymers: intensifying interfacial adhesion between the fibre and the matrix. *RSC Adv* 8(40):22729–22736
- Wang Z, Dai Q, Porter D (2016) Investigation of microwave healing performance of electrically conductive carbon fiber modified asphalt mixture beams. *Constr Build Mater* 126:1012–1019
- Zou G, Zhang D, Dong C (2006) Carbon nanofibers: synthesis, characterization, and electrochemical properties. *Carbon* 44(5):828–832

Publisher's Note Springer Nature remains neutral with regard to jurisdictional claims in published maps and institutional affiliations.